Chapter 17

Polycationic Probe-Guided Nanopore Single-Molecule Counter for Selective miRNA Detection

Kai Tian, Ruicheng Shi, Amy Gu, Michael Pennella, and Li-Qun Gu

Abstract

MicroRNAs (miRNAs) are a class of noncoding RNAs that are being explored as a new type of disease biomarkers. The nanopore single-molecule sensor offers a potential noninvasive tool to detect miRNAs for diagnostics and prognosis applications. However, one of the challenges that limits its clinical applications is the presence of a large variety of nontarget nucleic acids in the biofluid extracts. Upon interacting with the nanopore, nontarget nucleic acids produce "contaminative" nanopore signals that interfere with target miRNA discrimination, thus severely lowering the accuracy in target miRNA detection. We have reported a novel method that utilizes a designed polycationic peptide–PNA probe to specifically guide the target miRNA migration toward the nanopore, whereas any nontarget nucleic acids without the probe bound is rejected by the nanopore. Consequently, nontarget species are driven away from the nanopore and only the target miRNA can be detected at low concentration. This method is also able to discriminate miRNAs with single-nucleotide difference by using PNA to capture miRNA. Considering the significance and impact of this substantial advance for the future miRNA detection in biofluid samples, we prepared this detailed protocol, by which the readers can view the experimental procedure, data analysis, and resulting explanation.

Key words Nanopore, miRNA (miRNA), Single molecule, Biosensor, Cancer, HIV-1 TAT peptide, PNA, Probe, Diagnostics, Nucleic acids

1 Introduction

The nanopore offers a single-molecule platform for developing the next generation of biosensors and exploring various life science problems [1–14]. The nanopore technology can be utilized for rapid and low-cost gene sequencing, because individual base identity can be read out through change of the electric current during gene fragment translocation in the nanopore [15–23]. The sensitivity of the nanopore has also been applied to analyze epigenetic biomarkers, such as DNA methylation [24] and gene damage [25]. Our recent effort has been to develop the nanopore sensor for the electric detection of microRNAs (miRNAs) [26, 27]. The motivation is that miRNAs are a class of noncoding RNAs playing

Eckart Bindewald and Bruce A. Shapiro (eds.), *RNA Nanostructures: Methods and Protocols*, Methods in Molecular Biology, vol. 1632, DOI 10.1007/978-1-4939-7138-1_17,

important roles in gene expression modulation [28–31]. Numerous research results have found that miRNAs are potential cancer biomarkers [32–40]. Aberrant expression of specific miRNAs in cells and biofluids is associated with cancer development. Our nanopore-based single-molecule counting approach for circulating miRNA detection would offer a potential noninvasive tool for cancer diagnostics.

However, current nanopore sensors have limitations with respect to detecting miRNAs directly from patient samples. One of the challenges is "contaminative signals" generated by nontarget nucleic acids in the samples. The RNA extraction from biofluids not only contains the target miRNAs, but also numerous nontarget nucleic acids species, such as miRNAs, mRNAs, and tRNAs. Due to their negative charge, all these nucleic acids species can be driven to interact with the nanopore and change its conductance under the voltage. In addition to linear-form single-stranded and hybridized double-stranded nucleic acids, RNAs can also fold into tertiary structures that may clog the nanopore. Overall, the signals produced by nontarget nucleic acids can severely interfere with the accuracy of target miRNA detection. Accurate detection of miRNA in complex biological samples demands a method that enables the nanopore to only selectively capture the target miRNA, but reject any nontarget nucleic acids from entering the nanopore.

We have recently invented a polycationic probe guiding approach that can completely overcome this challenge [41]. Briefly we designed a polycationic probe as a cargo to specifically guide the migration of the target miRNA toward an engineered nanopore, whereas any nontarget species without probe binding migrates away from the nanopore driven by the voltage. Consequently, we can only observe signature signals of the target miRNA binding with the probe, but not any signals of nontarget nucleic acids. The probe comprises a short polycationic peptide linked to a peptide nucleic acid (PNA). The PNA is used to specifically capture target miRNA, while the polycationic peptide is a leader that guides the miRNA to be captured by the nanopore. Considering the broad application value and the important nanobiophysics mechanism of this method, we prepared this short protocol to introduce the detailed experimental procedure, including nanopore formation, nanopore current recording, signal analysis, and miRNA quantification, with a discussion on accuracy, sensitivity, specificity, versatility, multiple detection, and broad impact of the approach.

2 Materials

2.1 Reagents and Consumables

1. Pretreatment solution: 1:10 hexadecane–pentane. Mix 250 μL hexadecane with 2.5 mL pentane.

2. Lipid solution: 10 mg/mL. Dissolve 25 mg 1,2-diphytanoyl-sn-glycero-phosphocholine (Avanti Polar Lipids) in 2.5 mL pentane.
3. Nucleic acids stock solution: 1 mM. Dissolve synthetic miRNAs including miRNA *let 7a*, *7b*, or *7c* in RNAase-free water to 1 mM respectively.
4. Peptide–PNA probes corresponding to the miRNAs of interest (P_{7b} etc.) (*see* **Note 1**).
5. Recording solution: 0.5, 1, or 3 M KCl, buffered with 10 mM Tris and titrated with 1M HCl to pH 7.2.
6. α-hemolysin protein: 10–100 ng per 50 μL. Dissolve the K131D protein with ddH_2O.
7. Restriction enzymes: *EcoN* I or *Hind* III.
8. Expand Long Template PCR Synthesis Kit (Roche Diagnostic GmbH).
9. Coupled in vitro Transcription and Translation kit (IVTT, Promega).
10. XL10-gold super-competent *E. coli* cells.
11. Rabbit blood cell membrane (rabbit blood from Pel-Freez Biologicals).
12. Micron centrifugal filters that enable the concentration of biomolecules with a with a membrane nominal molecular weight limit (NMWL) of 10 kDa.

2.2 Setup and Instrument

1. Preparation of the chamber.
   (a) Compartments. Fabricate two Teflon compartments. Each compartment has a volume of 0.2–2 mL depending on specific design.
   (b) Partition. Prepare a piece of 25-μm thick Teflon film (Goodfellow) as partition and puncture a 100–150 μm wide tiny aperture in the center of the film. The lipid bilayer membrane will span over the aperture.
   (c) Chamber assembling. The chamber is assembled by tightly clicking the partition with two compartment blocks as shown in Fig. 1a. Seal the partition–compartment interface with vacuum grease. The cells on both sides of the partition are named *cis* and *trans*. The chamber is placed on the chamber holder, which has been preinstalled with two stirring motors under the bottom of the two cells for stirring. The chamber and the holder are placed in a Faraday box for shielding.
2. A pair of electrodes. Fabricate the Ag–AgCl electrode by merging a 0.5- or 1-mm wide silver wire in bleach overnight. A qualified electrode should have a dark brown surface. Fill 1.5%

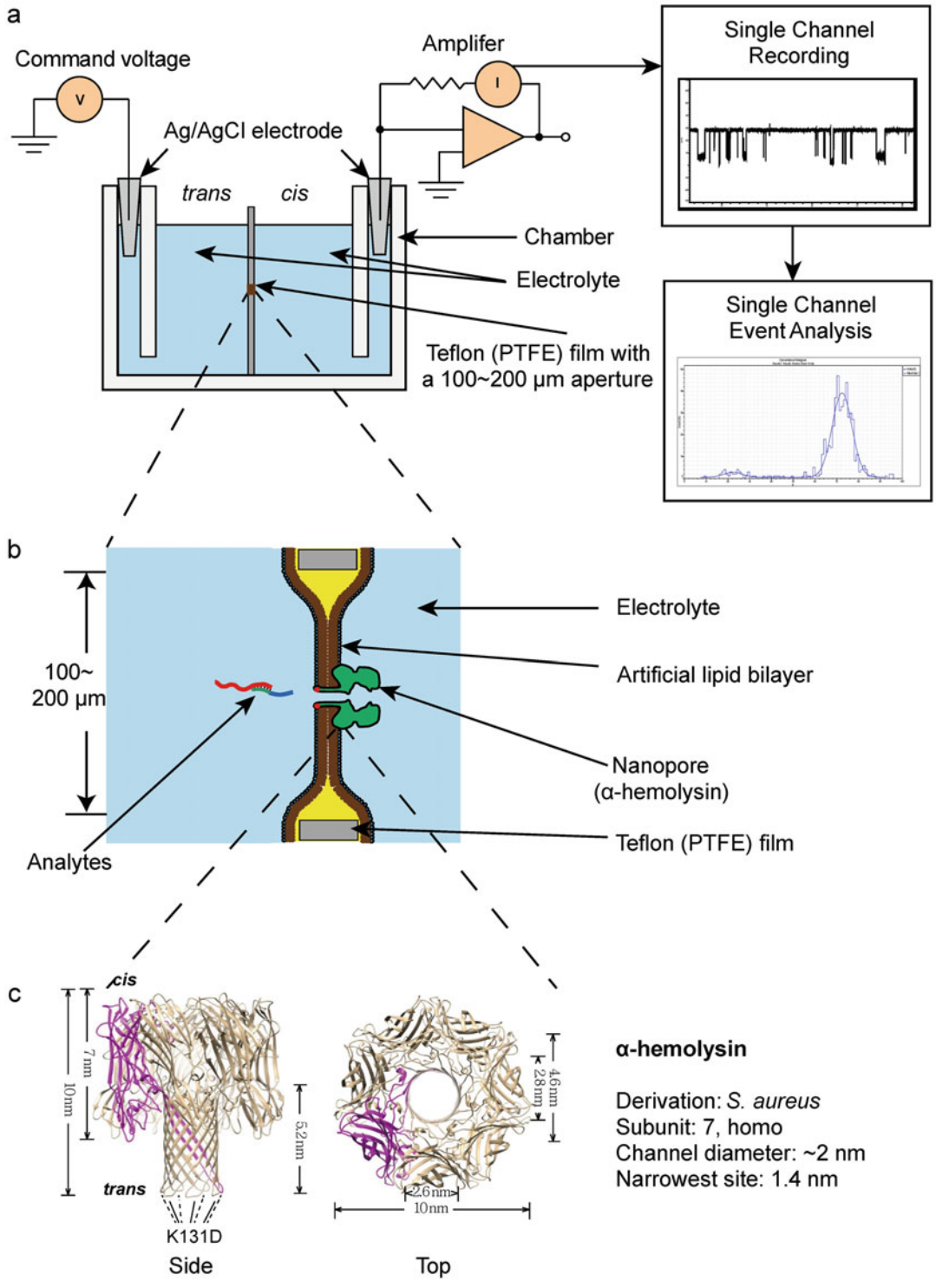

Fig. 1 Diagrams showing the lipid bilayer/protein pore experimental setup and components for electrical detection of miRNA in the engineered nanopore. (**a**) Schematic of experimental setup, including chamber, electrode, and amplifier (*left*). Nanopore current trace and analysis are also shown on the *right*. (**b**) Artificial lipid bilayer with a single nanopore embedding covers the aperture of Teflon film. (**c**) The structure of α-hemolysin nanopore and the engineered site in this method

agarose resolved in 3 M KCl in a 50 μL plastic pipette tip and fix the electrode in the gel.

3. Pico-Ampere current amplifier, used for recording ion current through the nanopore. The amplifier should be able to record pico-Ampere (ideally sub-pico-Ampere) currents.
4. Analog-to digital (AD) converter, used for acquiring the nanopore current data from the amplifier and for communicating the data to a computer. The AD converter should have a resolution of at least 16 bits and be capable of utilizing a sample rate of 250 kHz.
5. Computer that is compatible with the AD converter as well as software for data acquisition and analysis.

3 Methods

3.1 αHL Mutagenesis and Nanopore Purification

1. The K131D mutant αHL can be constructed using site-directed mutagenesis [42]. Digest the wild-type αHL plasmid by *EcoN* I or *Hind* III, respectively, into a linear template for PCR.
2. Add 20–30 ng linearized plasmid DNA and 200 pmol each of a nonmutagenic and a mutagenic primer with Expand Long Template PCR Synthesis Kit to 50 μL PCR mixture.
3. Perform PCR in the following temperature condition: 94 °C >5 min; 20 cycles of 94 °C 1 min, 50 °C 1 min, and 72 °C 3 min; 72 °C 6 min.
4. The two long PCR fragments, each from an enzyme digestion product, contain two overlapping sequences. Extract PCR fragments from the agarose gel.
5. Mix extracted PCR fragments.
6. Transform into XL10-gold super-competent *E. coli* cells, to form recombinant plasmid.
7. Extract mutant plasmid from *E. coli* cells.
8. Synthesize the K131D αHL protein using Coupled in vitro Transcription and Translation kit by following the protocol of the kit.
9. A 25 μL reaction contains 4 μL DNA template (400 ng/μL in stock solution) and complete amino acid mixture (including [^{35}S]methionine) in IVTT components, and is incubated at 37 °C for 1 h to produce protein monomers.
10. Mix the supernatant of the reaction with rabbit blood cell membrane to assemble the protein heptamer.
11. Separate the assembled heptameric protein by electrophoresis on a 7.5% SDS–polyacrylamide gel.

12. Cut out the oligomeric protein band.
13. Dissolve the gel band in 500 μL water.
14. Collect the protein using a micron centrifugal filter.
15. Divide the protein solution into ten aliquots, and store at −20 °C.

3.2 Nanopore Formation

1. Formation of lipid bilayer. Drop 2–5 μL of pretreatment solution by a 10 μL micropipette over the aperture of Teflon film, and immediately blow to dry. This aids in the formation a stable lipid bilayer.
2. Put a stirring bar into each cell of the chamber and place the chamber on the holder.
3. Connect the chamber to the amplifier through a pair of Ag–AgCl electrodes. Voltage provided by the amplifier is applied through the *trans* electrode; the *cis* cell is grounded.
4. Form the lipid bilayer according to the monolayer folding process described in ref. 43: inject 0.1–1 mL recording solution into each cell (0.2–2 mL), then drop 5 μL of lipid solution by a micropipette onto the surface of the solution.
5. Wait for 2–3 min to evaporate the pentane so as to form a molecular monolayer on the solution surface.
6. Gently inject another 0.1–1 mL recording solution from the bottom of each cell. The liquid surfaces on both sides are raised over the aperture of the partition. Immediately, the lipid monolayers on both sides automatically hybridize and form a bilayer membrane covering the aperture.
7. Use the data acquisition software to monitor capacitance and current thermal noise during membrane formation. A qualified lipid bilayer for a single channel recording should have a membrane resistance of ~100 GΩ, a capacitance of ~100–200 pF, and a current noise of 1.2–1.8 pA (the value of I_{RMS} on the amplifier panel).
8. Insertion of nanopore in the lipid bilayer. Upon bilayer formation, release 0.5–2 μL of protein solution to the *cis* solution close to the bilayer.
9. Gently stir the recording solution, while monitoring the current using data acquisition software. After a short time (tens of seconds to several minutes), the current suddenly increases sharply from zero to a specific level at a holding voltage, such as ~180 pA at +120 mV for K131D αHL, which indicates the insertion of a single nanopore in the lipid bilayer. Upon insertion, the wide entrance (nanocavity) of the pore faces the *cis* solution, while the narrow entrance (β-barrel) faces the *trans* solution (*see* the nanopore orientation in Fig. 1b).

3.3 Simultaneous Enrichment and Detection of miRNAs with a Polycationic Probe

1. Probe–miRNA hybridization. The probe P_{7b} contains a 10-base PNA sequence designed to specifically hybridize with miRNA Let-7b. The PNA was extended at the N-terminal with an 11-amino acid HIV-1 TAT polycationic peptide [44], which includes eight positively charged amino acids (six arginines and two lysines) (Fig. 2a). The P_{7b} and Let-7b mixture is added in *trans* solution (*see* **Notes 1** and **2**).
2. Observation of single probe–miRNA molecules. Apply a positive voltage, such as +180 mV, from the *trans* side to the grounded *cis* side and record the current using the data acquisition software. This voltage polarity can drive cationic molecules toward the pore while repelling anionic molecules away from the pore (*see* **Notes 3** and **4**).
3. Analysis of the signals. P_{7b} alone in *trans* solution shows a large number of Level-1 blocks (Fig. 2b). The duration of these blocks (τ_{off}) was 4.8 ms and their relative conductance I_R/I was 8.2% (I_R and I are currents of the block and the empty pore Fig. 2b). When the P_{7b} and miRNA Let-7b mixture is added in *trans* solution, a large number of distinct Level-2 blocks appear, while Level-1 blocks diminish. Compared with the Level-1 blocks, the Level-2 blocks were sixfold longer with a mean duration of 28 ± 4 ms and featured higher relative conductance at 26% (Fig. 2b). Therefore the Level-2 blocks serve as signatures for Let-7b identification. The occurring frequency of the signature signals generated by the P_{7b}·Let-7b complex (f_{sig}, the number of signature blocks per second) is linearly correlated with the Let-7b concentration, i.e., $f_{sig} \approx k_{on}$·[Let-7b], where k_{on} is the capture rate of the P_{7b}/Let-7b complex and [Let-7b] is the target miRNA concentration. Thus, f_{sig} is used to quantify miRNA concentration. f_{sig} corresponds to measuring the intervals between adjacent signature blocks using the software. τ_{sig} is obtained by fitting the histogram of all interval values to an exponential distribution function:

$$f(t) = Ae^{-t/\tau}$$

The inverted τ_{sig} is f_{sig}, i.e., $f_{sig}=1/\tau_{sig}$ (*see* **Note 5**).

4. Quantification of miRNAs. Repeat the P_{7b}/Let-7b experiments described above in a series of miRNA concentrations, such as 50 pM, 500 pM and 5 nM. Make a calibration curve using the set of f_{sig} at each concentration. The concentration of an unknown Let-7b sample can be determined according the calibration curve (*see* **Note 6**).

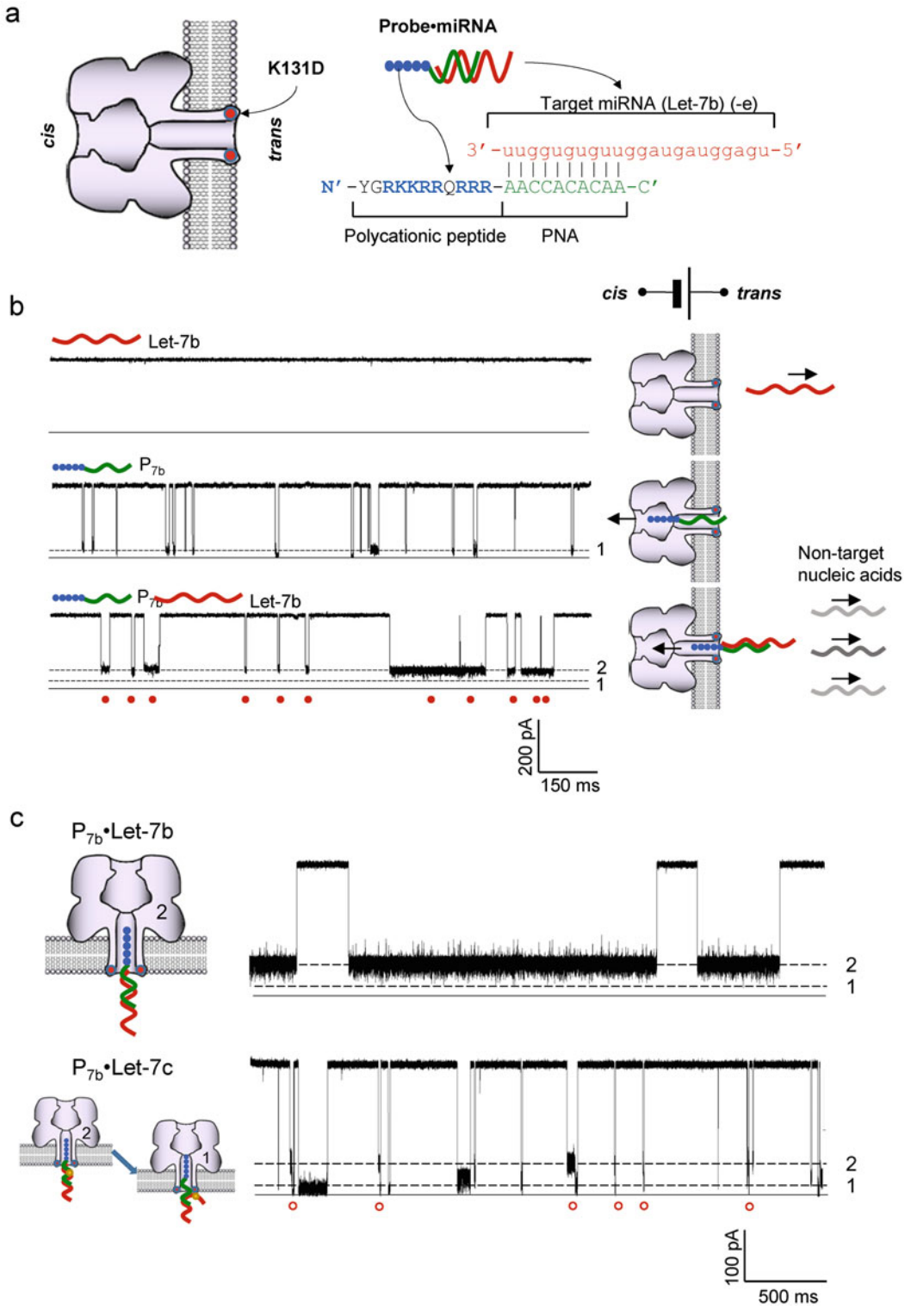

Fig. 2 Polycationic probe-guided specific detection of miRNA using the K131D protein nanopore. (**a**) Diagram showing cartoon of the *trans* opening of K131D with a group of negatively charged residues engineered around the *cis* entrance (*red dots* at the end of stem represent the negatively charged aspartic acids), and the

4 Notes

1. Polycationic probe. The polycationic probe is the key to guide the selective capture of target miRNA species. As shown in Fig. 2a, the probe is a peptide–PNA conjugate. PNA is used to capture miRNA, and the polycationic peptide is the leader that enables the nanopore to attract the probe·miRNA complex and guide its capture by the nanopore. The peptide leader is not necessary long, but need contain high density of positively charged amino acids to generate driving force near the nanopore entrance. The peptide–PNA copolymer can be synthesized (commercially available) at once without additional chemical cross-linking, as peptide and PNA have the same backbone. The sequence of the peptide leader is programmable. Its properties can be tuned by changing the peptide length and the number, position, and type of charged amino acids. The peptide can also be functionalized in any position of the sequence by chemical modification (such as cross-linking at cysteine), making it possible to generate unique signatures for multiplex detection.
2. Multiplex detections. This method has potential to be developed for multiplex detections, in which multiple target miRNAs as a biomarker panel can be simultaneously detected using one nanopore. Specific cancer diagnostics requires accurate detection of a biomarker panel that consists of multiple miRNAs. But currently one nanopore is only used to detect one miRNA. We have developed barcoded DNA probes for simultaneous detection of multiple miRNAs in one nanopore [27]. We designed a series of barcode probes to encode different targets. When the probe binds with the target, the barcode group such as polyethylene glycol attached on the probe can

Fig. 2 (continued) structures (sequences) of the polycationic probe, miRNA (Let-7b), and the probe–miRNA hybrid. The probe contains a HIV-1 TAT polycationic peptide (cationic Lys and Arg residues are marked in *blue*) and PNA sequence complementary to Let-7b sequence (marked in *green*). The sequence of miRNA Let-7b is marked in *red*; (**b**) (*Upper*) current trace of K131D pore showing that no block was observed in the presence of miRNA (Let-7b). (*Middle*) Current trace of K131D pore showing that the polycationic probe (P_{7b}) alone generated a large number of Level-1 blocks. (*Lower*) Current trace showing a large number of new Level-2 blocks (*solid red dots*) that were generated by the probe·miRNA hybrid (P_{7b}·Let-7b) in the presence of the miRNA (Let-7b) and its probe (P_{7b}). Models of suggested molecular processes are illustrated on the *right* of traces. Traces were recorded at +180 mV in 1 M KCl and 10 mM Tris (pH 7.2); (**c**) (*Upper*) Current traces and cartoon model showing characteristic blocks generated by the P_{7b}·Let-7b hybrid that is fully matched. (*Lower*) Current traces and cartoon model showing characteristic blocks generated by the P_{7b}·Let-7c hybrid that contains a single mismatched base pair (*lower*). Both blocks can be discriminated from the Level-1 block duration and the unzipping signature of the Level-2 terminal of the block (*hollow red dots*). Traces were recorded at +130 mV in 3 M/0.5 M (*cis*/*trans*) asymmetric solutions

specifically modulate the pore's ion flow. The resulting signature serves as a marker for the encoded target, and counting different signatures allows simultaneous analysis of multiple targets in one pore. This approach was verified by using a panel of lung cancer-derived miRNAs as the target. Supported by these result, we can develop barcoded polycationic peptide–PNA probes to simultaneously detect multiple cancer-derived miRNAs in one nanopore. Specifically, the polycationic peptide sequence can contain a cysteine at a designated position, and various chemical groups can be attached to cysteine to generate specific blocking levels when the probe is trapped in the nanopore. Each miRNA will be driven by a barcoded carrier probe that can generate a distinct signature for target recognition. As a result, multiple miRNAs can be quantified by counting their distinct signatures in one pore.

3. Versatility. We have developed the polycationic probe guiding method to selectively detect miRNA in a complex mixture also containing nontarget species. The biophysical mechanism behind this nano-phenomenon is not the electrophoretic and the electroosmotic effect. The specific driving force comes from a short range (several nanometers) electrical field formed by a group of negatively charged residues engineered around the *trans* entrance of the K131D pore. This field can only generate an attractive driving force on the polycationic peptide of the probe, but has much less repulsive force acting on the attached miRNA. Therefore the net force on the probe·miRNA complex remains attractive. Our unpublished data indicates that this method is also applicable to long nucleic acids by using a probe that has the same polycationic peptide head as we used for miRNA detection. We expect that this biophysical mechanism can be utilized to selectively capture any gene fragment, long or short, in complex samples that contain a large number of nontarget species.
4. Significance and broad impact. (1) The single-molecule counting method described here has the potential to become a new player to meet clinical needs for the detection of miRNA and other noncoding RNAs. The system is highly sensitive, specific, label-free, without need of amplification or secondary detection, fast (<1 h), inexpensive, simple to operate, and offers a multiplex detection. It may provide higher accuracy than PCR in assaying of patient samples [26]. For example, it could potentially become a new platform to develop a confirmatory test when the lung nodule is identified by low-dose helical computed tomography (LDCT) in high risk populations for lung cancer screening. The validated nanopore technology could be applied to detect any pathogenic DNA/RNA, single nucleotide polymorphism (SNP), and epigenetics such as DNA

methylation, for early diagnosis, prediction of cancer metastasis, and monitoring of response to therapy and thus could have a broad impact. Notably, the nanopore's SNP discrimination capability can be used not only to distinguish the family members of miRNA but also to detect a point mutation of the oncogene DNA in blood (circulating nuclear acids) that holds a huge potential for the early detection and monitoring of cancer. (2) The method we described in this report represents a substantial step toward medical applications of the nanopore. Unlike traditional electrophoretic and electroosmotic driving that lack selectivity, the polycationic guiding approach we invented provides a new route to nanopore selective capture of any nucleic acids target in a mixture for noise-free detection. Therefore for the first time it becomes possible to translate the nanopore sensor into a clinically usable tool. (3) The lipid bilayer supported protein nanopore system is not stable enough for clinical samples. There are three strategies to resolve the problem. First, whole DNAs or RNAs can be extracted from samples to avoid the contact between lipid bilayer and "membrane breakers" in the samples. Second, more solid supported systems are available now in several companies, such as Oxford Nanopore Technologies. Third, hybrid nanopores, i.e. combined solid and protein nanopores, may provide a new way to improve the stability of nanopore systems in clinical use [4]. Our long-term vision is to provide a compact, durable, and reliable nanopore device for performing rapid, accurate, low-cost, and high-throughput assays in a clinical diagnostic setting. If this method can be validated, we would be able to selectively and sensitively detect any type of nucleic acids, DNAs or RNAs, long or short, in complex clinical samples. The outcome will open a new avenue with significance not only in cancer detection and other human disease molecular diagnostics, but more broadly in fields such as plant science and foodborne detection where rapid genetic detection is required.

5. Accuracy and specificity. The most unique and useful advantage of this polycationic probe guiding method is that the probe (peptide–PNA) can guide the target miRNA to migrate toward the nanopore and is detected, whereas any nontarget nucleic acid species that are not binding with the probe migrate away from the nanopore without generating any "contaminative" or interference signals. As a result of this "noise-free" detection, only target miRNA signals are specifically generated and accurately recognized. We have used this method to test the mixture of target miRNA and various nontarget RNA and DNA. It has been found that the capture rate for the target miRNA alone and that in the mixture are the same, suggesting the

accuracy of this method. The specificity of this method is reflected by the capability to discriminate single-base differences between miRNAs with similar sequence, such as the Let-7 miRNA family. For example, the probe P_{7b} has been designed to detect Let-7, and can form fully matched hybrid P_{7b}·Let-7b. When P_{7b} hybridizes with another miRNA Let-7c, which has one-base difference from Let-7b, the hybrid P_{7b}·Let-7c forms a single mismatched base pair. Recorded in 3 M/0.5 M *cis/trans* KCl (pH 7.2) asymmetric solution at +130 mV. The duration of Level-2 signature of fully hybridized P_{7b}·Let-7b was 2.3 s (Fig. 2c), suggesting that P_{7b}·Let-7b is so stable that it cannot be unzipped prior to release from the pore. In contrast, the P_{7b}·Let-7c hybrid containing one mismatch generates a distinct type of two-level block from Level 2 to Level 1 (Fig. 2c). The Level-2 signature was only 19 ms, about 120 times shorter than Level-2 blocks for P_{7b}·Let-7b; and the terminal Level-1 block corresponds to the unzipping of the hybrid followed by translocation of the probe through the pore, suggesting that one mismatch induced in a RNA–PNA duplex can greatly reduce its stability. Overall, different stabilities of RNA–PNA hybrids without and with mismatch can generate distinct signatures that can be utilized to discriminate single-base difference in miRNAs.

6. Sensitivity. The K131D mutant pore, which has been engineered with a ring of anionic aspartic acids at the *trans* opening, plays an important role in attracting cationic molecules. It greatly increases the target capture rate k_{on}. The P_{7b}·Let-7b complex was rarely trapped in the wild type, while its k_{on} was 80 ±9 $\mu M^{-1}\ s^{-1}$ in the K131D. Also, it is much higher than the k_{on} for the miRNA in complex with a DNA probe, which was reported as 1.4 $\mu M^{-1}\ s^{-1}$ [26]. Therefore the combination of the polycationic probe and the engineered nanopore enhance k_{on} over 50-fold. The frequency of P_{7b}/Let-7b signatures consistently increases with increasing Let-7b concentrations ranging from 50 pM to 5 nM at +180 mV. It can be fitted to a straight line in the log–log scale. Therefore, Let-7b can be detected as low as tens of picomolar. Note that the K131D pore itself may spontaneously generate blocks [45], but the occurrence is very low (~$6 \times 10^{-3}\ s^{-1}$ above +140 mV), and its current pattern (amplitude) is different from the signature of the probe·miRNA complex. Therefore, the background noise signal from the pore itself can be excluded.

Acknowledgment

We appreciate Amy Gu and Michael Pennella who contributed to the nanopore experiments as highschool student research trainees.

This work was supported through initial NSF CAREER award 0546165 and NIH R01-GM079613, and current NIH R01-GM114204. This investigation was conducted in a facility constructed with support from the Research Facilities Improvement Program Grant C06-RR-016489-01 from the National Center for Research Resources, National Institutes of Health.

References

1. Bayley H et al (2008) Droplet interface bilayers. Mol Biosyst 4(12):1191–1208
2. Bayley H, Jayasinghe L (2004) Functional engineered channels and pores (Review). Mol Membr Biol 21(4):209–220
3. L-Q G, Shim JW (2010) Single molecule sensing by nanopores and nanopore devices. Analyst 135(3):441–451
4. Hall AR et al (2010) Hybrid pore formation by directed insertion of [alpha]-haemolysin into solid-state nanopores. Nat Nanotechnol 5 (12):874–877
5. Hornblower B et al (2007) Single-molecule analysis of DNA-protein complexes using nanopores. Nat Methods 4(4):315–317
6. Howorka S, Siwy Z (2009) Nanopore analytics: sensing of single molecules. Chem Soc Rev 38(8):2360–2384
7. Langecker M et al (2012) Synthetic lipid membrane channels formed by designed DNA nanostructures. Science 338(6109):932–936
8. Ma L, Cockroft SL (2010) Biological nanopores for single-molecule biophysics. ChemBioChem 11(1):25–34
9. Majd S et al (2010) Applications of biological pores in nanomedicine, sensing, and nanoelectronics. Curr Opin Biotechnol 21(4):439–476
10. Movileanu L (2009) Interrogating single proteins through nanopores: challenges and opportunities. Trends Biotechnol 27(6):333–341
11. Olasagasti F et al (2010) Replication of individual DNA molecules under electronic control using a protein nanopore. Nat Nanotechnol 5 (11):798–806
12. Venkatesan BM, Bashir R (2011) Nanopore sensors for nucleic acid analysis. Nat Nanotechnol 6(10):615–624
13. Wanunu M, Morrison W, Rabin Y, Grosberg AY, Meller A (2010) Electrostatic focusing of unlabelled DNA into nanoscale pores using a salt gradient. Nat Nanotechnol 5(2):160–165
14. Wendell D et al (2009) Translocation of double-stranded DNA through membrane-adapted phi29 motor protein nanopores. Nat Nanotechnol 4(11):765–772
15. Branton D et al (2008) The potential and challenges of nanopore sequencing. Nat Biotechnol 26(10):1146–1153
16. Cherf GM et al (2012) Automated forward and reverse ratcheting of DNA in a nanopore at 5-A precision. Nat Biotechnol 30(4):344–348
17. Kasianowicz JJ, Brandin E, Branton D, Deamer DW (1996) Characterization of individual polynucleotide molecules using a membrane channel. Proc Natl Acad Sci U S A 93(24):13770–13773
18. Manrao EA et al (2012) Reading DNA at single-nucleotide resolution with a mutant MspA nanopore and phi29 DNA polymerase. Nat Biotechnol 30(4):349–353
19. Ashton PM et al (2015) MinION nanopore sequencing identifies the position and structure of a bacterial antibiotic resistance island. Nat Biotechnol 33(3):296–300
20. Bolisetty MT, Rajadinakaran G, Graveley BR (2015) Determining exon connectivity in complex mRNAs by nanopore sequencing. Genome Biol 16(1):1–12
21. Laszlo AH et al (2014) Decoding long nanopore sequencing reads of natural DNA. Nat Biotechnol 32(8):829–833
22. Norris AL, Workman RE, Fan Y, Eshleman JR, Timp W (2016) Nanopore sequencing detects structural variants in cancer. Cancer Biol Ther 17(3):246–253
23. Quick J et al (2016) Real-time, portable genome sequencing for Ebola surveillance. Nature 530 (7589):228–232
24. Wallace EVB et al (2010) Identification of epigenetic DNA modifications with a protein nanopore. Chem Commun 46(43):8195–8197
25. An N, Fleming AM, White HS, Burrows CJ (2012) Crown ether–electrolyte interactions permit nanopore detection of individual DNA abasic sites in single molecules. Proc Natl Acad Sci U S A 109(29):11504–11509
26. Wang Y, Zheng D, Tan Q, Wang MX, L-Q G (2011) Nanopore-based detection of circulating microRNAs in lung cancer patients. Nat Nanotechnol 6(10):668–674
27. Zhang X, Wang Y, Fricke BL, L-Q G (2014) Programming nanopore ion flow for encoded

multiplex microRNA detection. ACS Nano 8 (4):3444–3450
28. Carthew RW, Sontheimer EJ (2009) Origins and mechanisms of miRNAs and siRNAs. Cell 136(4):642–655
29. Kim VN, Han J, Siomi MC (2009) Biogenesis of small RNAs in animals. Nat Rev Mol Cell Biol 10(2):126–139
30. Lee RC, Feinbaum RL, Ambros V (1993) The C. elegans heterochronic gene lin-4 encodes small RNAs with antisense complementarity to lin-14. Cell 75(5):843–854
31. Wightman B, Ha I, Ruvkun G (1993) Post-transcriptional regulation of the heterochronic gene lin-14 by lin-4 mediates temporal pattern formation in C. elegans. Cell 75(5):855–862
32. Boeri M et al (2011) MicroRNA signatures in tissues and plasma predict development and prognosis of computed tomography detected lung cancer. Proc Natl Acad Sci U S A 108 (9):3713–3718
33. Hu Z et al (2010) Serum microRNA signatures identified in a genome-wide serum microRNA expression profiling predict survival of non-small-cell lung cancer. J Clin Oncol 28 (10):1721–1726
34. Hunt EA, Goulding AM, Deo SK (2009) Direct detection and quantification of microRNAs. Anal Biochem 387(1):1–12
35. Iorio MV, Croce CM (2009) MicroRNAs in cancer: small molecules with a huge impact. J Clin Oncol 27(34):5848–5856
36. Landi MT et al (2010) MicroRNA expression differentiates histology and predicts survival of lung cancer. Clin Cancer Res 16(2):430–441
37. Mitchell PS et al (2008) Circulating microRNAs as stable blood-based markers for cancer detection. Proc Natl Acad Sci U S A 105 (30):10513–10518
38. Shen J et al (2011) Plasma microRNAs as potential biomarkers for non-small-cell lung cancer. Lab Invest 91(4):579–587
39. Sozzi G et al (2009) Plasma DNA quantification in lung cancer computed tomography screening. Am J Respir Crit Care Med 179 (1):69–74
40. Zheng D et al (2011) Plasma microRNAs as novel biomarkers for early detection of lung cancer. Int J Clin Exp Pathol 4(6):575–586
41. Tian K, He Z, Wang Y, Chen SJ, LQ G (2013) Designing a polycationic probe for simultaneous enrichment and detection of microRNAs in a nanopore. ACS Nano 7(5):3962–3969
42. Howorka S, Bayley H (1998) Improved protocol for high-throughput cysteine scanning mutagenesis. Biotechniques 25(5):764–766, 768, 770 passim
43. Montal M, Mueller P (1972) Formation of bimolecular membranes from lipid monolayers and a study of their electrical properties. Proc Natl Acad Sci U S A 69(12):3561–3566
44. Takeshima K, Chikushi A, Lee K-K, Yonehara S, Matsuzaki K (2003) Translocation of analogues of the antimicrobial peptides magainin and buforin across human cell membranes. J Biol Chem 278(2):1310–1315
45. Mohammad MM, Movileanu L (2010) Impact of distant charge reversals within a robust beta-barrel protein pore. J Phys Chem B 114 (26):8750–8759